

Bound and Quasibound States of He_2H^+ and He_2D^+ †

Aditya Narayan Panda and N. Sathyamurthy*,‡

Department of Chemistry, Indian Institute of Technology Kanpur 208 016, India

Received: January 31, 2003; In Final Form: March 14, 2003

Bound and quasibound states of He_2H^+ and He_2D^+ in three dimensions have been computed by use of a time-dependent quantum-mechanical wave packet approach for total angular momentum $J = 0$. Seven bound states were found for He_2H^+ and 14 for He_2D^+ , as compared to five for both systems by Lee and Secrest (*J. Chem. Phys.* **1986**, 85, 6565). The potential energy surface needed for the dynamical calculation has been computed by carrying out an ab initio calculation with coupled cluster single and double excitations with perturbative triple excitations [CCSD(T)] employing d-aug-cc-PVTZ basis set. A many-body expansion function proposed by Aguado et al. (*Comput. Phys. Commun.* **1998**, 108, 259) was fitted to the ab initio potential energy values and the resulting fit has a root-mean-square deviation of 10.8 meV (0.25 kcal/mol).

1. Introduction

Rare gas dimers (X_2) are known to be weakly bound species,^{1–4} held together by weak van der Waals interaction. Helium dimer, the weakest among them, has a binding energy of only 0.957 meV.² However, they become highly stable in the presence of a proton. Using the afterglow technique, Adams et al.⁵ observed the formation of XH^+ and X_2H^+ , when they reacted H_2 with X_2^+ .

Valence bond calculations for He_2H^+ by Poshusta et al.⁶ yielded a linear symmetric structure with H–He length (r_e) of 1.70 a_0 and a vibrational frequency of 1400 cm^{-1} . Poshusta and Siems⁷ carried out a valence bond configuration interaction (VBCI) calculation and reported a linear symmetric equilibrium structure with $r_e = 1.764 a_0$. Milleur et al.⁸ performed an SCF-LCAO-MO calculation and found the linear symmetric He_2H^+ to be stable with $r_e = 1.75 a_0$ and a potential well of 0.5757 eV with respect to the asymptotically separated HeH^+ and He. They reported the potential energy surface for collinear He_2H^+ and selected nonlinear configurations. Dykstra⁹ carried out self-consistent electron pair (SCEP) and double substituted coupled cluster (CCD) calculations, which confirmed the linear symmetric structure of He_2H^+ and showed r_e to be 1.746 and 1.747 a_0 , respectively. While studying protonated rare gas clusters, Baccarelli et al.¹⁰ employed multireference single and double excitations with configuration interaction (MRD-CI) calculations with cc-PVTZ basis set to examine the H^+ insertion into the cluster from linear and nonlinear approaches. The symmetric insertion of the proton yielded the most strongly bound configuration for the protonated helium dimer. The equilibrium geometry corresponded to $r_e = 1.75 a_0$ and $D_e = 0.52$ eV. Filippone and Gianturco¹¹ carried out a classical molecular dynamics study, which confirmed the symmetric linear structure of the He_2H^+ complex. A systematic study of the He_2H^+ system was carried out recently by Kim and Lee¹² using second- and fourth-order Møller–Plesset perturbation theory (MP2, MP4) and coupled cluster with single and double excitations with perturbative triple excitations [CCSD(T)] approach with

TABLE 1: Equilibrium Bond Length and Dissociation Energy for He_2H^+ as Determined by Various Theoretical Studies

| method | $r_e (a_0)$ | $D_e (\text{eV})$ |
|------------------------|-------------|-------------------|
| VB ⁶ | 1.70 | 0.96 |
| VBCI ⁷ | 1.764 | 0.456 |
| LCAO – MO ⁸ | 1.75 | 0.5757 |
| SCF ⁹ | 1.749 | 0.49 |
| SCEP ⁹ | 1.746 | 0.571 |
| CCD ⁹ | 1.747 | 0.5757 |
| MRDCI ¹⁰ | 1.75 | 0.52 |
| CCSD(T) ¹² | 1.748 | 0.5741 |
| present [CCSD(T)] | 1.75 | 0.578 |

6-311++G(d,p),(3df,3pd) and aug-cc-PVxZ(x=D,T,Q) basis sets. A summary of the findings of the different theoretical studies is given in Table 1.

Most of the above-mentioned studies have focused on the equilibrium geometry and well depth. Dykstra⁹ did compute the potential energy values for a limited number of geometries around the minimum, and an analytic functional fit to those values were obtained by Lee and Secrest.¹³ Understandably, their fit was accurate near the minimum and was *not* dependable for extended configurations. Baccarelli et al.¹⁰ examined the potential energy surface (PES) for collinear $[\text{He}–\text{H}–\text{He}]^+$ and $[\text{He}–\text{He}–\text{H}]^+$ geometries and for C_{2v} geometries of $[\text{He}–\text{H}–\text{He}]^+$. Although they did not report an analytic fit of their PES, they showed that the lowest-lying excited electronic state (charge-transfer channel) is 11.15 eV above the ground state in the asymptotic region and much higher in the Franck–Condon region for the equilibrium geometry of He_2H^+ . The only other extensive study of the system was by Kim and Lee,¹² who also examined only a limited region of the configuration space. Therefore, there was an acute need for an accurate PES over extended configurations of He_2H^+ in its ground electronic state.

To the best of our knowledge, there is only one report on the bound states of He_2H^+ . Lee and Secrest,¹³ using the PES reported by Dykstra,⁹ performed variational and perturbative calculations to determine the rotation–vibration states of He_2H^+ and He_2D^+ for total angular momentum $J = 0, 1, 2$. Five bound states were found for both He_2H^+ and He_2D^+ for $J = 0$. They had also acknowledged that their results were less dependable at energies far removed from the minimum. Because of their

† Part of the special issue “Donald J. Kouri Festschrift”.

* To whom correspondence should be addressed: e-mail nsath@iitk.ac.in.

‡ Honorary Professor, Jawaharlal Nehru Centre for Advanced Scientific Research, Jakkur, P.O., Bangalore 560064, India.

abundance in interstellar medium and in ionized gases, it would be worthwhile to compute the bound states of He_2H^+ and its isotopomer.

Therefore we have undertaken to compute the ab initio PES for He_2H^+ over an extended range of geometries, fitted an analytic function to it and computed the bound states of He_2H^+ and He_2D^+ using a time-dependent quantum-mechanical wave packet methodology. In section 2.1 we describe the method used to calculate the potential energy data points. Section 2.2 describes the theoretical methodology used to calculate the bound and quasibound states of He_2H^+ and He_2D^+ . In section 3 we discuss the features of the PES and present the bound state results. We summarize our findings in section 4.

2. Methodology

2.1. Potential Energy Surface. To study the structure and stability of the He_2H^+ system in its ground electronic state, the potential energy surface was generated by use of the MOLPRO suite of programs.¹⁴ The CCSD(T) method was used with correlation consistent basis set d-aug-cc-PVTZ to compute the points on the PES. The dissociation energy (D_e) was calculated by means of the supermolecule approach as

$$D_e = -[E(\text{He}_2\text{H}^+) - E(\text{HeH}^+) - E(\text{He})] \quad (1)$$

where $E(\text{He})$, $E(\text{HeH}^+)$, and $E(\text{He}_2\text{H}^+)$ represent the energies for each species at the optimized geometries.

2.2. Bound and Quasibound State Calculation. The time-dependent quantum-mechanical wave packet method used for computing bound and quasibound states is well documented in the literature.^{15–18} We have adopted the same for computing the bound and quasibound states of He_2H^+ and He_2D^+ . The Hamiltonian¹⁹ for a triatomic system (A, BC) with total angular momentum $J = 0$ in the body-fixed (BF) frame is given by

$$\begin{aligned} \hat{H} = & \frac{1}{2} \left[\frac{P_R^2}{\mu_R} + \frac{P_r^2}{\mu_r} \right] + \frac{\mathbf{j}^2}{2I} + V(R, r, \theta) \\ = & -\frac{\hbar^2}{2} \left[\frac{1}{\mu_R} \frac{\partial^2}{\partial R^2} + \frac{1}{\mu_r} \frac{\partial^2}{\partial r^2} \right] - \frac{\hbar^2}{2I} \frac{1}{\sin \theta} \frac{\partial}{\partial \theta} \left(\sin \theta \frac{\partial}{\partial \theta} \right) + \\ & V(R, r, \theta) \quad (2) \end{aligned}$$

where P_R and P_r are the momentum operators corresponding to the two Jacobi distances R and r , respectively, and θ is the angle between R and r . \mathbf{j} is the rotational angular momentum operator for $\text{BC}[\text{HeH}(\text{D})^+]$, μ_r is the $\text{BC}[\text{HeH}(\text{D})^+]$ reduced mass, μ_R $[=m_{\text{He}}(m_{\text{H}(\text{D})} + m_{\text{He}})/(m_{\text{He}} + m_{\text{H}(\text{D})} + m_{\text{He}})]$ is the $[\text{He}, \text{H}(\text{D})\text{He}^+]$ reduced mass, and I is the moment of inertia of the system defined as $1/I = 1/(\mu_R R^2) + 1/(\mu_r r^2)$. The body-fixed z axis is taken to be parallel to R , and BC lies in the xz plane. $V(R, r, \theta)$ is the three-body interaction potential.

The initial wave packet $\Psi(t=0)$ is taken to be a Gaussian located in the interaction region of the PES used in the calculation. In terms of the equally spaced grid points R_l and r_m along R and r , respectively, and the nodes (θ_n) of a 29-point Gauss–Legendre quadrature (GLQ)²⁰ along θ

$$\begin{aligned} \Psi(R_l, r_m, \theta_n, t=0) = & N \sqrt{w(n)} \exp \left[-\frac{(R_l - R_0)^2}{2\sigma_R^2} - \frac{(r_m - r_0)^2}{2\sigma_r^2} \right] \times \\ & \left\{ \exp \left[-\frac{(\theta_n - \theta_0)^2}{2\sigma_\theta^2} \right] + \exp \left[-\frac{(\theta_n - \pi + \theta_0)^2}{2\sigma_\theta^2} \right] \right\} \quad (3) \end{aligned}$$

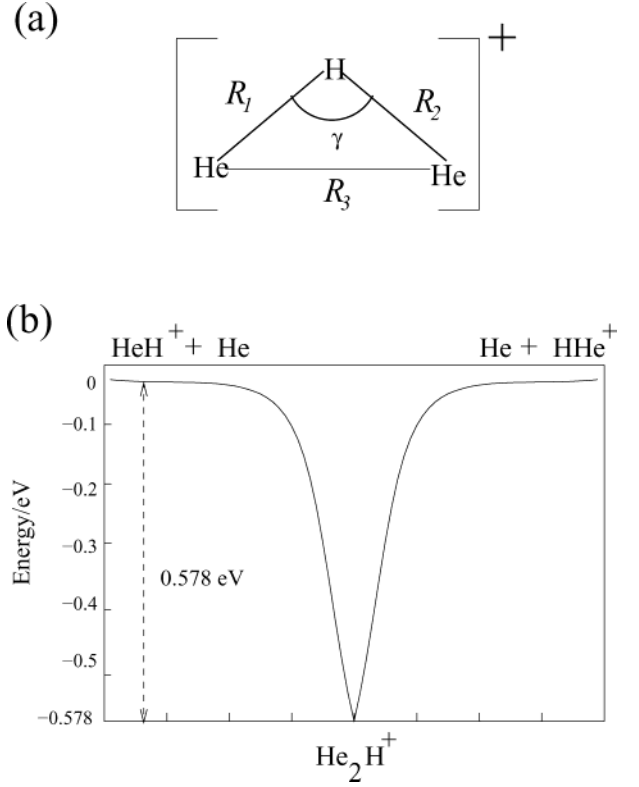


Figure 1. (a) Coordinate system used for computing the PES. (b) Potential energy profile for the rearrangement $\text{HeH}^+ + \text{He} \rightarrow \text{He} + \text{HHe}^+$ in collinear geometry.

TABLE 2: Eigenvalues (in eV) Corresponding to the Bound States of Three-Dimensional He_2H^+ and He_2D^+ for $J = 0$, with Zero Energy Corresponding to Well-Separated He and $\text{H}(\text{D})\text{He}^+$

| He_2H^+ | | He_2D^+ | |
|---------------------------|--------------|---------------------------|--------------|
| variational ¹³ | TDQM/present | variational ¹³ | TDQM/present |
| -0.2927 | -0.3092 | -0.3465 | -0.3596 |
| -0.1733 | -0.1909 | -0.2250 | -0.2436 |
| -0.0749 | -0.1405 | -0.2336 | -0.2260 |
| -0.0573 | -0.1019 | -0.1185 | -0.2021 |
| +0.0117 | -0.0773 | -0.0805 | -0.1423 |
| | -0.0456 | | -0.1188 |
| | -0.0105 | | -0.1054 |
| | | | -0.0966 |
| | | | -0.0667 |
| | | | -0.0562 |
| | | | -0.0409 |
| | | | -0.0345 |
| | | | -0.0181 |
| | | | -0.0023 |

where N is the normalization constant, $\sqrt{w(n)}$ is the GLQ weight, and σ_R , σ_r , and σ_θ are the width parameters of the Gaussian wave packet (GWP) along the respective coordinates. The initial location of the GWP is given by R_0 , r_0 , and θ_0 .

The wave function $\Psi(t)$ at time t is obtained by time-evolving the wave packet by use of the split-operator algorithm²¹ for a large number (N_T) of small time steps (Δt) as

$$e^{-i\hat{H}\Delta t/\hbar} = e^{-iV\Delta t/2\hbar} e^{-iT\Delta t/4\hbar} e^{-iT\Delta t/\hbar} e^{-iT\Delta t/4\hbar} e^{-iV\Delta t/2\hbar} + O(\Delta t^3) \quad (4)$$

where $T = (P_R^2/2\mu_R + P_r^2/2\mu_r)$, is the total radial kinetic energy operator. The action of the exponential operator in T is carried out via the fast Fourier transform (FFT) algorithm.^{21,22} To evaluate the exponential involving rotational kinetic energy

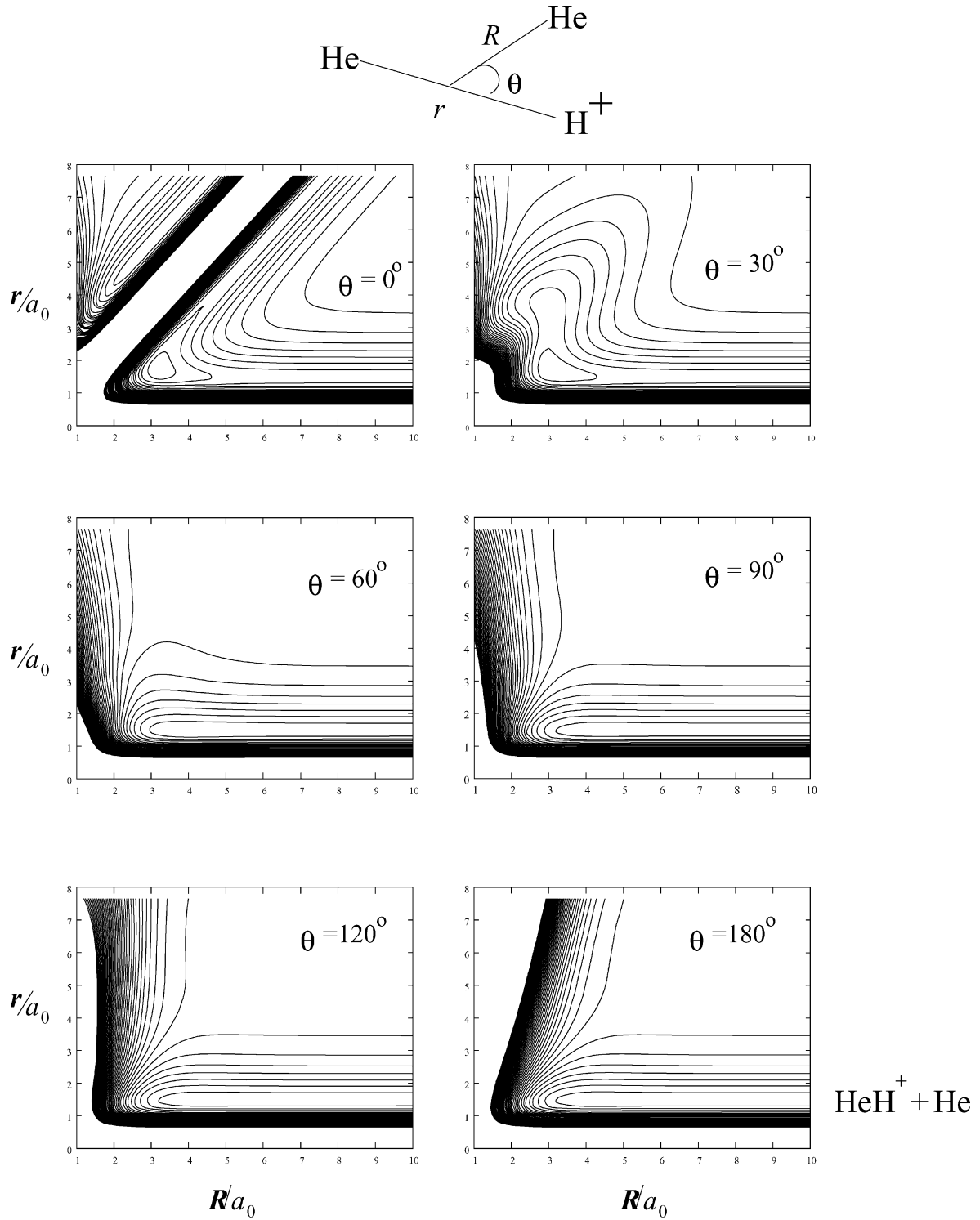


Figure 2. Potential energy contour diagram for the ground electronic state of He_2H^+ in (R, r) space for different values of θ indicated in the panel. Successive contours differ by 0.2 eV, with zero energy corresponding to $\text{HeH}^+ + \text{He}$.

operator, $e^{-i\hat{p}^2\Delta t/4\hbar}$, we have used the discrete variable representation (DVR)^{23,24} along with the GLQ.

The power spectrum $I(E)$ is obtained by Fourier-transforming the autocorrelation function $C(t) = \langle \Psi(0) | \Psi(t) \rangle$:

$$I(E) = \left| \int_0^\infty C(t) e^{iEt/\hbar} dt \right|^2 \quad (5)$$

We utilized the time-reversal property of $\Psi(t)$ to calculate the autocorrelation function at time $2t$ by evaluating

$$C(2t) = \langle \Psi^*(t) | \Psi(t) \rangle \quad (6)$$

from the wave function at time t . This approach^{25,26} allows us to increase the energy resolution ($\Delta E = 2\pi\hbar/\tau$) by a factor of 2 by effectively doubling the total propagation time τ .

The eigenfunctions $\Psi(E_n)$ for the system are calculated by projecting the time-evolved wave function onto the desired eigenstate (n) of energy E_n :

$$\Psi(E_n) = \int_0^\infty \Psi(t) e^{iE_n t/\hbar} dt \quad (7)$$

As the wave packet moves forward in time, the fast-moving components approach the grid edges ahead of the slow-moving

ones. Hence, to get rid of the possible unphysical wraparounds from the edges of a finite sized grid, we multiplied the wave function at each time step by a damping function:^{27,28}

$$f(X_i) = \sin\left[\frac{\pi}{2} \frac{X_{\text{mask}} + \Delta X_{\text{mask}} - X_i}{\Delta X_{\text{mask}}}\right] \quad X_i \geq X_{\text{mask}} \quad (8)$$

where X_{mask} is the point at which the damping function is initiated along the channel coordinate X (R or r) and $\Delta X_{\text{mask}} (= X_{\text{max}} - X_{\text{mask}})$ is the width of X over which the function decays from 1 to 0, with X_{max} being the maximum value of X .

3. Results and Discussion

3.1. Potential Energy Surface. As mentioned above, we computed the points on the ground-state PES of He_2H^+ by the CCSD(T) method with d-aug-cc-PVTZ basis set. Potential energy values were calculated for the $[\text{He}-\text{H}-\text{He}]^+$ angle $\gamma = 0(30)180^\circ$ and for the two He-H distances R_1 and $R_2 = 1(0.2)10.0 a_0$. The variables are defined in Figure 1a.

An analytic functional fit to the computed ab initio potential energy values was obtained by the many-body expansion method of Aguado et al.²⁹ The potential energy function for a triatomic system is written as

$$V_{\text{ABC}}(R_1, R_2, R_3) = V_A^{(1)} + V_B^{(1)} + V_C^{(1)} + V_{\text{AB}}^{(2)}(R_1) + V_{\text{BC}}^{(2)}(R_2) + V_{\text{AC}}^{(2)}(R_3) + V_{\text{ABC}}^{(3)}(R_1, R_2, R_3) \quad (9)$$

The diatomic potential for AB is given by

$$V_{\text{AB}}^{(2)} = \frac{c_0 \exp(-\alpha_{\text{AB}} R_1)}{R_1} + \sum_{i=1}^L c_i \rho_1^i \quad (10)$$

Similar expressions hold for BC and CA.

Rydberg type variables ρ_i are given by

$$\rho_i = R_i \exp(-\beta_i R_i) \quad (11)$$

The three-body term $V_{\text{ABC}}^{(3)}$ is written as

$$V_{\text{ABC}}^{(3)}(R_1, R_2, R_3) = \sum_{ijk}^M d_{ijk} \rho_1^i \rho_2^j \rho_3^k \quad (12)$$

Compared to the computed ab initio potential energy values, the fitted surface gave a root-mean-square deviation of 10.8 meV (0.25 kcal/mol).

The resulting potential energy profile for the collinear configuration is shown schematically in Figure 1b. In Figure 2 we plot the potential energy contour diagram in the (R, r) plane for the various values of θ . Figure 3a shows the potential energy contours as a He atom approaches HeH^+ in its equilibrium geometry, and Figure 3b depicts the contours for the approach of a proton toward He_2 in its equilibrium geometry.

As was shown in Table 1, the location and depth of the well computed by us are comparable to the results reported by Dykstra.⁹ Unfortunately, we are not able to make a detailed comparison of our PES with that of Dykstra, as he did not report all the energy values. For the limited number of geometries for which the potentials are reproduced in ref 9, we have compared our potential energy values with his and found a standard deviation of 21.08 meV, with the largest deviations being +45.3 and -47.2 meV. The analytic fit reported by Lee and Secrest

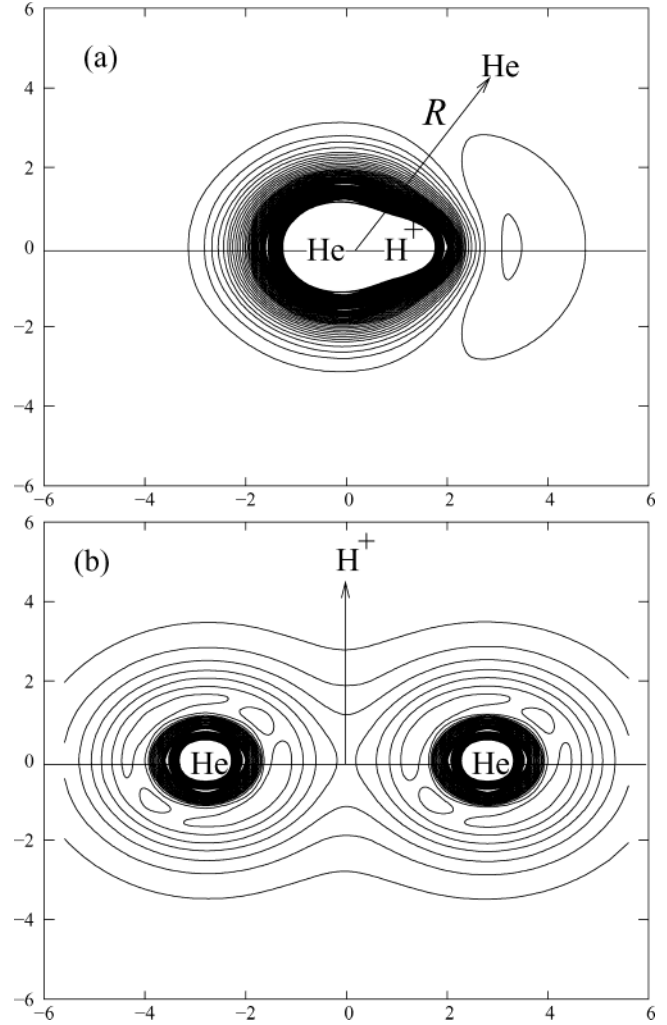


Figure 3. (a) Potential energy contour diagram for the approach of a He atom toward HeH^+ in its equilibrium geometry. Successive contours differ by 0.2 eV. (b) Potential energy contour diagram for a proton approaching He_2 in its equilibrium geometry. Successive contours differ by 0.2 eV.

gives only a limited amount of information and is known to be less reliable as one moves away from the minimum.

3.2. Bound and Quasibound States Calculation. The initial wave function was centered at $(R_0, r_0, \theta_0) = (4.00 a_0, 1.8 a_0, 0.212754 \text{ rad})$ and the width parameters $\sigma_R = 0.30 a_0$, $\sigma_r = 0.25 a_0$, $\sigma_\theta = 0.20 \text{ rad}$. The time evolution of the wave function was carried out on a $64 \times 64 \times 29$ grid in (R, r, θ) for a total of 32 768 time steps with each step $\Delta t = 0.2155 \text{ fs}$. The damping function used $R_{\text{mask}} = 7.48 a_0$, $r_{\text{mask}} = 7.48 a_0$. The autocorrelation function was computed with the Simpson integration and Fourier-transformed by use of the FFT algorithm. The resulting eigenvalue spectrum for three-dimensional He_2H^+ is plotted in Figure 4a, with the inset showing only the bound states. There are a total of seven bound states and their energies are listed in Table 2. These are to be compared with the five bound states reported by Lee and Secrest¹³ using a variational calculation and a slightly different PES. The currently computed zero-point level is lower than that reported by Lee and Secrest by 21.7 meV. For the purpose of quantitative comparison we report the energy levels (in reciprocal centimeters) relative to the zero-point energy, as was done by Lee and Secrest,¹³ in Figure 5a. These authors had pointed out that the energy levels did not correspond to any particular normal mode and that they could be identified as a linear combination of modes, because

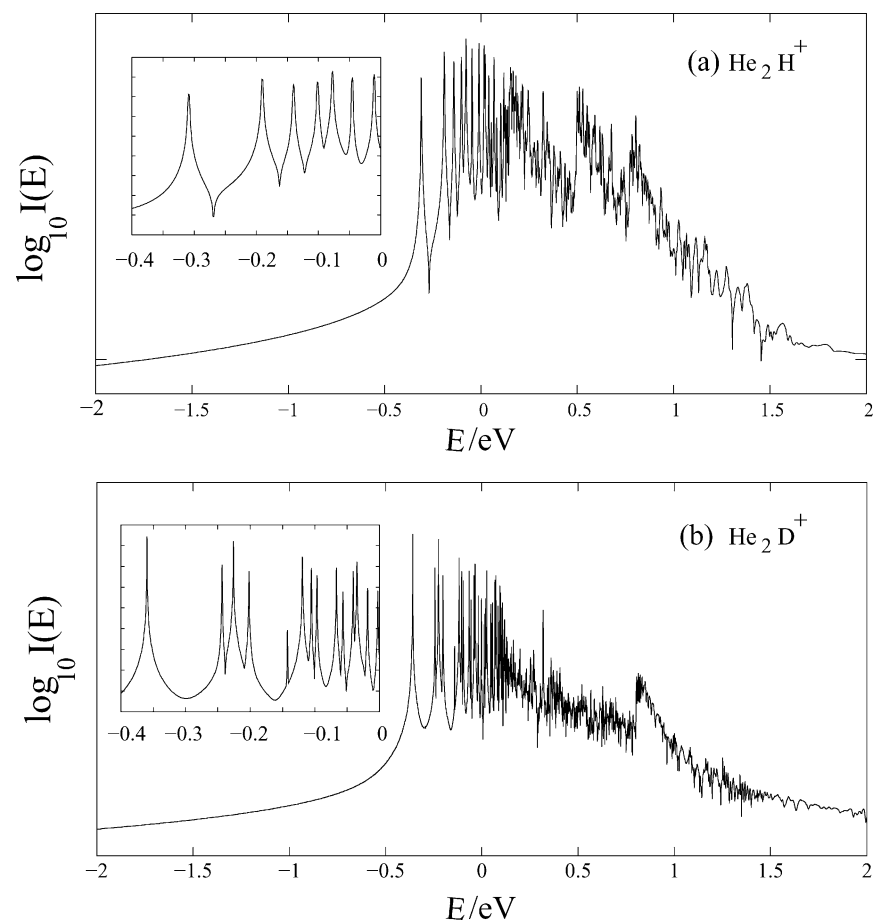


Figure 4. Eigenvalue spectra for (a) He_2H^+ and (b) He_2D^+ in three dimensions for $J = 0$. The insets show the bound states.

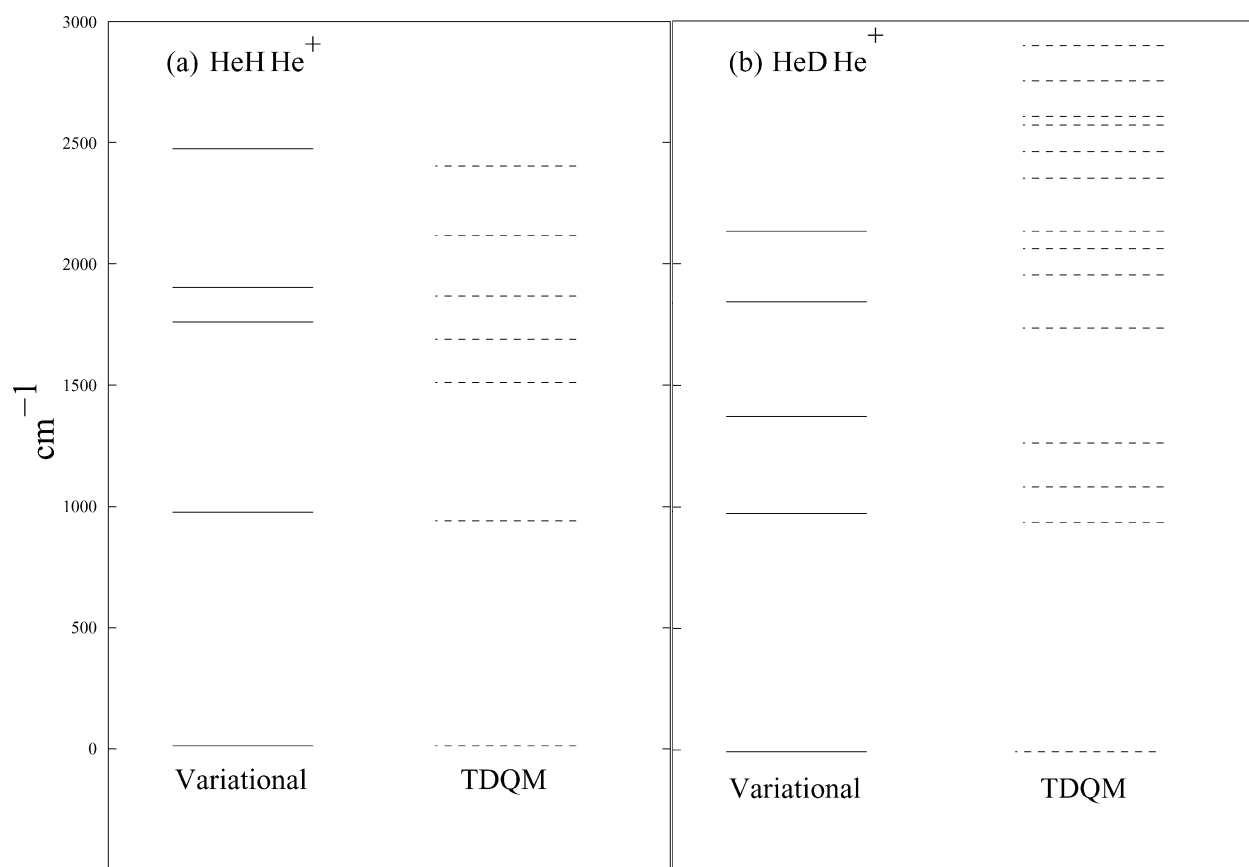


Figure 5. Bound-state energies computed from the present study along with those reported by Lee and Secrest¹³ for (a) He_2H^+ and (b) He_2D^+ .

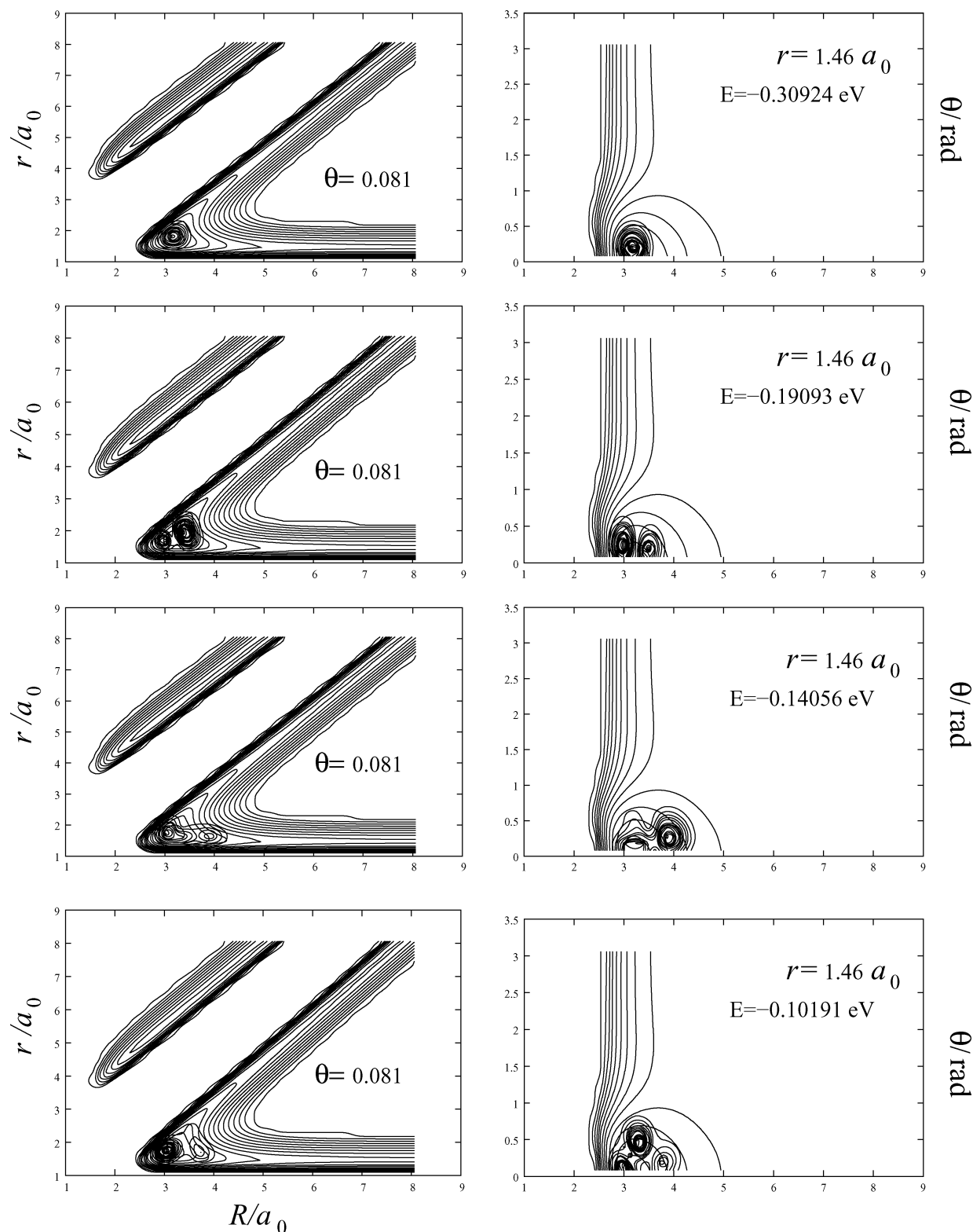


Figure 6. Probability density contours for the lowest four bound states of He_2H^+ , superimposed on the potential energy contours for the system.

of the floppiness of the molecule. The light H nucleus bound between the two heavy He nuclei makes large-amplitude motions. It is clear that the first excited state from our calculations is almost identical to that of Lee and Secrest.¹³ The deviations become larger as we go higher in energy. This is not surprising because Lee and Secrest¹³ used a normal mode expansion for fitting the PES and the data available away from the well region were limited and the fit was less reliable as one moved away from the minimum. Our PES covers a much wider

region in configuration space and has been fitted analytically with an rms deviation of 10.8 meV. Because of the anharmonicity of the potential, we do find a larger number of bound states than Lee and Secrest.¹³

Probability density contours of the eigenfunctions corresponding to the lowest four bound states in both (R, r) and (R, θ) coordinates, superimposed on the potential energy contours for the system, are reproduced in Figure 6. The lowest energy eigenfunction in Figure 6a could be assigned the quantum

numbers $(n_R, n_r, n_\theta) = (0, 0, 0)$. The eigenfunction in Figure 6b is predominantly that of the first excited vibrational state $(1, 0, 0)$. With an increase in energy, the nodal pattern becomes complicated and it becomes difficult to assign (n_R, n_r, n_θ) . This is understandable because of the floppiness of the system, as discussed above.

Although we have not analyzed the eigenvalue spectrum above zero energy, it is clear that it would correspond to the quasibound states and that the He_2H^+ system can be expected to be rich in dynamical resonances, akin to HeH_2^+ .¹⁶

The eigenvalue spectrum of He_2D^+ plotted in Figure 4b reveals 14 bound states, when compared to seven for He_2H^+ . Interestingly, Lee and Secrest¹³ reported only five bound states for He_2D^+ also. A quantitative comparison of the eigenvalues obtained by our study against those of Lee and Secrest is presented in Table 2 and in Figure 5b. Once again we have used the zero-point energy level as zero energy for comparing the two sets of results. While the first vibrationally excited state on our ab initio PES is in near quantitative agreement with that reported by Lee and Secrest, the differences between the two sets of results increase with increasing energy. On the basis of kinematic considerations one would have expected a larger number of bound states for He_2D^+ than for He_2H^+ . That is what we have found with our TDQM calculations.

Ideally, one would have liked to repeat our TDQM calculations with the Lee–Secrest PES to identify the source of the discrepancy between the results obtained on the two surfaces. Unfortunately, the Lee–Secrest PES is not available in a readily usable form. An alternative is to compute the bound states supported by the newly computed ab initio PES by an alternative approach such as BOUND³⁰ or DVR.³¹ But considering the success of the TDQM method for a variety of other systems,¹⁸ we feel that this is not needed, particularly because (i) the larger number of bound states obtained for He_2H^+ and He_2D^+ on our surface can be readily attributed to the anharmonicity of the PES and (ii) the larger number of bound states for He_2D^+ than that for He_2H^+ on our surface is what one expects from kinematic considerations.

4. Summary and Conclusion

We have reported a CCSD(T) potential energy surface for the ground state of three-dimensional He_2H^+ and also an analytic fit to it with an rms deviation of 10.8 meV (0.25 kcal/mol). The computed eigenvalue spectrum for the system for $J = 0$ shows seven bound states for He_2H^+ and 14 for He_2D^+ , compared to five reported earlier for both the systems. We have found that there is a large number of quasibound states that would suggest that He_2H^+ and He_2D^+ systems would be rich in dynamical resonances.

Acknowledgment. We would like to thank Professor Biman Bagchi (IISc, Bangalore) for pointing out the importance of

He_2H^+ and Professor Franco Gianturco (University of Rome, Italy) for sharing his earlier results on the system with us. We are grateful to Pavel Soldan (University of Durham, England) for useful discussions and to the anonymous reviewers for their valuable comments on an earlier version of the manuscript.

References and Notes

- (1) Grisenti, R. E.; Schollkopf, W.; Toennies, J. P.; Hegerfeldt, G. C.; Kohler, T.; Stoll, M. *Phys. Rev. Lett.* **2000**, *85*, 2284.
- (2) Tang, K. T.; Toennies, J. P.; Yiu, C. L. *Phys. Rev. Lett.* **1997**, *74*, 1546.
- (3) Cybulski, S. M.; Toczytowski, R. R. *J. Chem. Phys.* **1999**, *111*, 10520.
- (4) Tao, F. *J. Chem. Phys.* **1999**, *111*, 2407.
- (5) Adams, N. G.; Bohme, D. K.; Ferguson, E. E. *J. Chem. Phys.* **1970**, *52*, 5101.
- (6) Poshusta, R. D.; Haugen, J. A.; Zetik, D. F. *J. Chem. Phys.* **1969**, *51*, 3343.
- (7) Poshusta, R. D.; Siems, W. F. *J. Chem. Phys.* **1971**, *50*, 1995.
- (8) Milleur, M. B.; Matcha, R. L.; Hayes, E. F. *J. Chem. Phys.* **1974**, *60*, 674.
- (9) Dykstra, C. E. *J. Mol. Struct.* **1983**, *103*, 131.
- (10) Baccarelli, I.; Gianturco, F. A.; Schneider, F. J. *Phys. Chem.* **1997**, *101*, 6054.
- (11) Filippone, F.; Gianturco, F. A. *Eur. Lett.* **1998**, *44*, 585.
- (12) Kim, S. T.; Lee, J. S. *J. Chem. Phys.* **1999**, *110*, 4413.
- (13) Lee, J. S.; Secrest, D. *J. Chem. Phys.* **1986**, *85*, 6565.
- (14) MOLPRO is a package of ab initio programs written by H.-J. Werner and P. J. Knowles with contributions from R. D. Amos et al.
- (15) Skodje, R. T.; Sadeghi, R.; Köppel, H.; Krause, J. L. *J. Chem. Phys.* **1994**, *101*, 1725.
- (16) Mahapatra, S.; Sathyamurthy, N. *J. Chem. Phys.* **1995**, *102*, 6057.
- (17) Balakrishnan, N.; Kalyanaraman, C.; Sathyamurthy, N. *Phys. Rep.* **1997**, *280*, 79.
- (18) Mahapatra, S.; Chakrabarti, N.; Sathyamurthy, N. *Int. Rev. Phys. Chem.* **1999**, *18*, 235.
- (19) Zhang, J. Z. H. *Theory and Application of Quantum Molecular Dynamics*; World Scientific: Singapore, 1999.
- (20) Press, W. H.; Flannery, B. P.; Teukolsky, S. A.; Vetterling, W. T. *Numerical Recipes: The Art of Scientific Computing*; Cambridge University Press: Cambridge, U.K., 1986.
- (21) Fleck, J. A.; Morris, J. R.; Feit, M. D. *Appl. Phys.* **1976**, *10*, 129.
- (22) Kosloff, D.; Kosloff, R. *J. Comput. Phys.* **1983**, *53*, 35.
- (23) Lill, J. V.; Parker, G. A.; Light, J. C. *Chem. Phys. Lett.* **1982**, *89*, 483.
- (24) Light, J. C.; Hamilton, I. P.; Lill, J. V. *J. Chem. Phys.* **1985**, *82*, 1400.
- (25) Manthe, U.; Meyer, H.-D.; Cederbaum, L. S. *J. Chem. Phys.* **1992**, *97*, 9062.
- (26) Engel, V. *Chem. Phys. Lett.* **1992**, *189*, 76.
- (27) Bisseling, R. H.; Kosloff, R.; Manz, J. *J. Chem. Phys.* **1985**, *83*, 993.
- (28) Mahapatra, S.; Sathyamurthy, N. *J. Chem. Soc., Faraday Trans.* **1997**, *93*, 773.
- (29) Aguado, A.; Tablero, C.; Paniagua, M. *Comput. Phys. Commun.* **1998**, *108*, 259.
- (30) Hutson, J. M. BOUND; CCP6 Program Library; University of Durham, England.
- (31) Tennyson, J.; Henderson, J. R.; Fulton, N. G. DVR3D; CPC Program Library.